PHYSICAL REVIEW B VOLUME 57, NUMBER 7 15 FEBRUARY 1998-I

X-ray absorption spectroscopy study of atomic structure of epitaxial $ErSi_{1.7}(0001)$ on Si(111)

R. Gunnella
Laboratoire d'Etudes des Propriétés Electroniques des Solides, CNRS, associé à l'Université Joseph Fourier,
Boîte Postale 166, 38042 Grenoble, France
and Dipartimento di Matematicae Fisica, Università degli Studi di Camerino,
sez INFM, via Madonna delle Carceri, 62032 Camerino (MC), Italy

J. Y. Veuillen and T. A. Nguyen Tan
Laboratoire d'Etudes des Propriétés Electroniques des Solides, CNRS, associé à l'Université Joseph Fourier,
Boîte Postale 166, 38042 Grenoble, France

A. M. Flank
LURE, Bâtiment 209D, Université Paris-Sud, 91405 Orsay, France

(Received 31 March 1997; revised manuscript received 12 September 1997)

The x-ray absorption near-edge spectra of the Si K edge were measured on $ErSi_{1.7}(0001)$, epitaxially grown on Si(111) at normal and glancing incidence angles of the light. The silicide films were prepared by coevaporation under ultrahigh vacuum, characterized by low-energy electron diffraction and photoemission and covered with a thin carbon protective layer before transferring to the synchrotron radiation facility. The Si K edge showed a strong dependence on the polarization of the light, denoting the different bonding characters of the p_{x-y} and the p_z Si final states. The experimental curves are compared to the ones calculated by the extended-continuum method for different possible configurations of the Si atoms in the silicide: stoichiometric $ErSi_2$; nonstoichiometric $ErSi_{1.7}$, where one out of six Si atoms of the hexagonal ring is missing; without and with relaxations of the Si and the Er atoms due to the presence of ordered Si vacancies. The presence of these vacancies is immediately evidenced by comparison between experimental and calculated absorption curves. The best agreement is obtained when relaxations of Er and Si atomic positions around the vacancies are taken into account. [S0163-1829(98)02407-2]

I. INTRODUCTION

It has been shown that erbium silicide thin films with good crystalline quality can be grown epitaxially on Si(111) substrates.[1,2] This metallic silicide can thus be considered as a model system for studying metal-semiconductor junctions.

Another remarkable property, common to rare earth silicides, is the low value of the Schottky barrier height (SBH) on n-type silicon (≈ 0.3 eV). Possible applications in silicon technology taking advantage of this low SBH have been proposed in literature.[3,4]

The crystallographic structure of the material under study is basically derived from the hexagonal AlB_2 one which consists of a stacking of alternate Er and Si planes along the (0001) direction. For epitaxial layers on Si(111), as in the present case, the (0001) direction is perpendicular to the film surface. In the stoichiometric AlB_2 phase, the composition of the silicide would be $ErSi_2$. However, it has been known long ago that the silicide has a significant amount of Si vacancies and that the actual composition is close to $ErSi_{1.7}$.[5,6] This composition corresponds to one out of six Si atoms missing in the Si planes. The vacancy ordering has been found to give several different superstructures.[6–8] A structural analysis by x-ray-diffraction (XRD) of the atomic positions in silicide thin epilayers with a $\sqrt{3}\times\sqrt{3}R(30°)$ ($R3$) superstructure has been published recently.[9] It shows a sizable relaxation of both Er and Si atoms around the Si vacancies.

The band structure and density of states (DOS) of bulk erbium silicide has been investigated by several groups.[10–13] A simple approach to the silicide electronic structure is the molecular model presented by Allan, Lefebvre, and Christensen.[12] For the stoichiometric $ErSi_2$ phase, the bonding within the Si plane can be considered as ‘‘graphitic-like’’ in a first approximation. The Si atoms form sp_2 bonds with their three nearest-neighbor Si atoms in the (0001) Si planes. It remains one Si $3p_z$ bond [the z axis is chosen parallel to the (0001) direction] normal to the Si planes, forming a π bond. In real materials, this schematic picture should be modified to take into account the presence of vacancies. Each vacancy generates three dangling bonds within the Si(0001) planes, and also induces relaxations of neighboring Si and Er atoms.[9] There is eventually a significant charge transfer from Er to Si atoms that results in the filling of the dangling-bond states on Si atoms.[12] More elaborate band-structure calculations have been proposed.[10–13] Comparison with experimental data[10,11,13] suggests that the silicide DOS changes significantly when vacancies are included in the structure, although some features, such as the energy location of the vacancy-induced states, remain unclear.[12,13] In any case, ambiguities remain, which are related to the nonstoichiometric nature of the silicide. The main problem is then to take properly into account the influence of the vacancies on the atomic and electronic structure of the material. X-ray absorption at the Si K edge on this compound in the near-edge range can give insights on the local order around Si atoms.

0163-1829/98/57(7)/4154(6)/$15.00

In this paper we present x-ray-absorption spectroscopy (XAS) experiments at the Si K edge of silicide layers epitaxially grown on Si(111) substrates. The first objective is to get information on the electronic structure of this compound by probing the Si $3p$ partial empty DOS. This complements previous works by photoemission and x-ray emission combined with electronic structure calculations.[10,14] From the bonding scheme described above, we can expect the Si $3p$ density of states to be anisotropic, with different contributions parallel and perpendicular to the z axis. By using the linear polarization of the synchrotron radiation, the p_z and p_{x-y} contributions can be probed independently. The second, and most important, objective is to investigate the local order around Si atoms by analyzing the experimental x-ray absorption near-edge spectra (XANES) using a multiple scattering approach. [An investigation of the local order using an extended x-ray absorption fine structure (EXAFS) analysis which is, in principle, easier is not possible for erbium silicide due to the presence of Er absorption lines in the EXAFS range.]

The presence of vacancies is clearly established in the present work, and the amounts of relaxation of Er and Si atoms around the vacancies can be compared with the values obtained from x-ray diffraction.[9]

The experimental details and the computational techniques are described in Secs. II and III, respectively. The results are presented and discussed in Sec. IV.

II. EXPERIMENT

Erbium silicide layers were grown on clean Si(111)-7 $\times 7$ surfaces in UHV conditions using a codeposition technique described previously.[2] Er and Si atoms were deposited simultaneously in the ratio of 1/1.7 on the substrate held at room temperature. The composition of the deposit was checked periodically by x-ray photoemission spectroscopy (XPS). Once the desired thickness, estimated by the evaporation rates, was attained, the film was annealed at 750 °C for about 20 min to induce epitaxial growth of the silicide. This technique has been shown to give films with smooth morphology, i.e., with a low density of pinholes, and good crystalline quality.[2] The films present sharp $R3$ low-energy electron diffraction patterns and characteristic XPS and Auger spectra of $ErSi_{1.7}(0001)$. Their composition, measured by Rutherford backscattering spectroscopy, was $ErSi_x$ with x ranging between 1.65 and 1.70. Two samples with thicknesses of 500 and 800 Å, as controlled by x-ray reflectivity measurements, were used obtaining very similar XAS results. The layers were capped *in situ* with a 10–15 Å-thick C layer to prevent a severe surface transformation during transfer to the experimental station. We verified that this procedure is very efficient for reducing the oxidation of the surface layer, by performing XPS measurements on capped and noncapped samples after the XAS experiments. The XAS experiments were performed at the Laboratoire pour l'Utilisation de Rayonnement Electromagnetique (LURE) on the SA32 beamline of the Super-ACO storage ring. The signal was collected in the total electron yield mode. The monochromator was fitted with InSb(111) crystals, giving an instrumental resolution of 0.7 eV at the Si K edge.

III. COMPUTATION

The x-ray absorption cross section of the Si K edge was calculated by means of a fully converged full multiple-scattering formalism with a Hedin-Lundqvist potential. The method employed is denominated extended continuum (EC) and described by Tyson and co-workers.[15] In this method bound and continuum final states of the photoelectron excited during the absorption of a photon of energy close to the electron binding energy, are considered to have the same analytical behavior in terms of the same kind of Bessel and Hankel functions, and are represented as propagating electronic waves in a piecewise potential, the muffin-tin potential constituted by atomic regions of spherical symmetry and by an interstitial constant potential. In the extended continuum method the interstitial constant potential is extended everywhere in the space and also electronic states with an energy greater than the interstitial potential but smaller than zero (i.e., bound states), are considered as propagating solution of the Schrödinger equation.

The advantage of this method is to consider bound states as very narrow scattering resonances ultimately leaking away from the cluster region in a continuum state, instead of decaying exponentially as true bound states do. In this way, the same single continuum calculation gives the energy separation between bound-state features and features of the continuum of the spectrum. This results to be very convenient; in fact, even if some slight variations are expected in the energy separation of the features appearing at the absorption edge, if a proper a self-consistent (SCF) potential is used, it is in general difficult to connect these bound states to those ones of the continuum calculated by the usual non-SCF approach. The EC method is in this way able to give an overview of the final density of states in the region of the absorption edge. Actually, the main drawback of this method is the error introduced in the normalization used for the final bound state which is the same as that used for the propagating states. This results in an underestimate of the bound-state transition strength.

SCF charge density and atomic X-α potentials were superimposed after spherical average to build the muffin-tin (MT) cluster potential used in the calculation. For the absorbing atom a completely relaxed $(Z+1)$ potential was used.

The MT radii were chosen slightly superimposed (8%) by means of a Norman criterion.[15] The exchange and correlation part of the potential was calculated following the method of Hedin and Lundqvist,[16] properly modified for atomic core regions.[15] The imaginary part of this potential controls the propagation and the damping of the excited photoelectron everywhere in the system in the approximation of a single local plasmon excitation in the solid during the photoelectron pathway, and is able to reproduce the observed mean free path in metals and semiconductors. Calculations were performed after convergence obtained for clusters of 200 atoms (radius of 9 Å). For this cluster the $ErSi_2$ ideal structure has been generated taking advantage of the $D3h$ symmetry. Starting from these clusters similar calculations have been done for a $ErSi_{1.7}$ structure, i.e., the ideal $ErSi_2$ with $\frac{1}{6}$ of the silicon atoms missing.

The latter calculations consists of two independent contri-

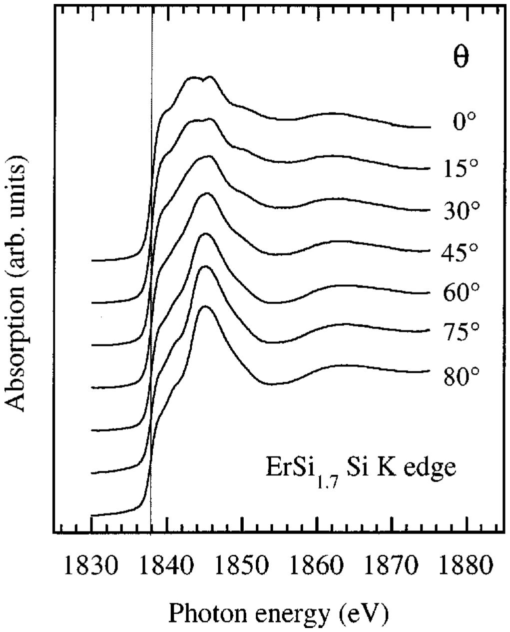

FIG. 1. X-ray-absorption spectra of an epitaxial erbium silicide layer in the Si K near-edge region. The spectra have been normalized at 1900 eV photon energy and shifted vertically for clarity. The thin vertical line is at the threshold energy. The incidence angle θ of the x-ray beam relative to the surface normal is indicated on the right side of each spectrum ($\theta = 0°$ normal incidence, $\theta = 80°$ grazing incidence).

butions, type I and type II, respectively, for the Si absorbing atoms having or not having a dangling bond due to the ejection of $\frac{1}{6}$ of Si atoms from the structure. For these two calculations it has taken advantage of a $C2v$ and $D3h$ symmetry, respectively. Finally, two calculations were done for two different relaxations of the $ErSi_{1.7}$ structure following the work of Lohmeier *et al.*[9] These two calculations are named $R1$ and $R2$, where $R2$ is exactly the relaxation optimized in the above reference,[9] with the silicon atoms moving toward the vacancies for 0.27 Å and the Er atoms retracting for 0.12 Å; for $R1$ the amount of displacements is reduced by 50%. The c-axis length used is 4.03 Å. A maximum value of $l = 3$ for the real spherical harmonics basis functions was used. Finally a convolution of the theoretical spectra was performed to take into account the finite lifetime of the Si K core hole (Lorentzian linewidth of 0.5 eV) and the experimental energy resolution (Gaussian linewidth of 0.7 eV).

IV. RESULTS AND DISCUSSION

The raw experimental data are shown in Fig. 1. The spectra have been collected for various incidence angles θ of the x-ray beam relative to the surface normal. With this notation, the $\theta = 0°$ spectrum probes the Si p_x and Si p_y partial DOS, whereas the spectrum at $\theta = 80°$ shows the Si p_z partial DOS of the silicide [the z axis is parallel to the (0001) direction and thus normal to the surface]. The nonzero angular acceptance of the radiation cone and some uncertitude in the position of the electrons orbit in the storage ring reduce the degree of linear polarization to around 90% at the sample. This nonperfect linear polarization should be taken into account in the analysis.

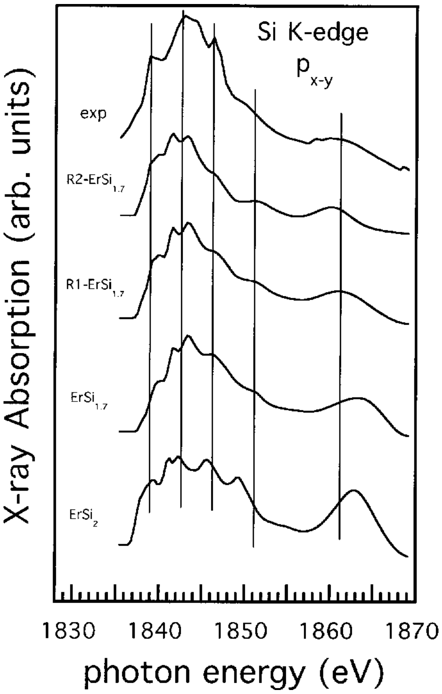

FIG. 2. p_{x-y} final state of $ErSi_{1.7}$ Si K XAS spectra: from the bottom curve is shown the near-edge absorption of $ErSi_2$, $ErSi_{1.7}$ without relaxation of the lattice parameters, and the $R1$-$ErSi_{1.7}$ and $R2$-$ErSi_{1.7}$ structures, respectively, with values of the relaxation 0.135 Å for the Si atoms moving toward the vacancies and 0.06 Å retraction of the Er atoms and 0.270 Å for the Si atoms moving toward the vacancies and 0.12 Å retraction of the Er atoms. The $R2$ structure is that optimized in Ref. 9. The top curve is the experimental XAS spectrum, taken with normal-incidence angle of the light.

Close to threshold, the contribution of the Si $3p$ states should be dominant. As mentioned in the Introduction, we expect a strong anisotropy between grazing and normal incidence spectra due to the ''graphitelike'' structure of the Si planes of the samples. This anisotropy clearly shows up in the experimental data of Fig. 1. However, the interaction with Er neighbors and the presence of the Si vacancies lead to polarized absorption spectra quite different from those of graphite[17] although the anisotropic character is preserved.

The energy of the absorption edge (thin vertical line in Fig. 1) is close, within ±1 eV, to the value of the Si $1s$ core-level binding energy (1838.8 ± 0.1 eV) as measured by XPS using a Zr L_α x-ray line. The uncertainty is mainly related to the calibration of the spectrometers. This suggests that both Si $3p_z$ and Si $3p_{x-y}$ contribute to the density of states at and right above the Fermi level, in agreement with theoretical results.[10,12] It is not possible to go further in the comparison of the spectra with the computed partial densities of states because the published data do not extend beyond 4 eV above the Fermi level.

We modeled the XANES spectra in a structure that consists of an ordered array of Si vacancies giving rise to a $R3$ superstructure in the (0001) planes. This model was similar to the one proposed in an XRD study by Lohmeier and co-workers.[9]

The amounts of relaxation of the Si and Er atoms around the vacancy were varied between 0 and the values reported in

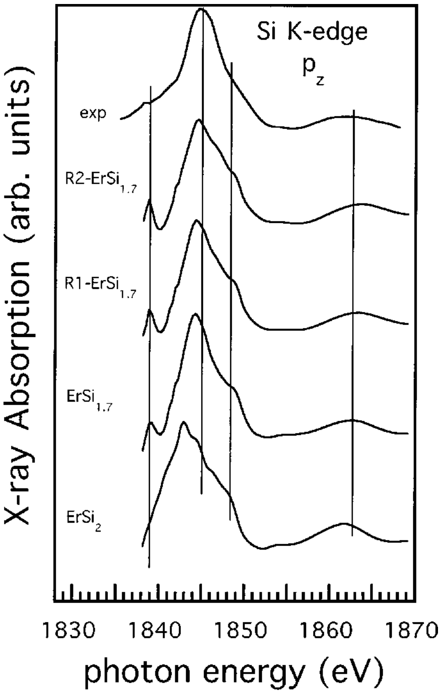

FIG. 3. As in Fig. 2 for the p_z final state of ErSi$_{1.7}$ Si K XAS spectra. The top curve is the experimental XAS spectrum, taken with $\theta = 80°$ incidence angle of the light.

Ref. 9. A computation has also been made for the stoichiometric ErSi$_2$ structure in order to check the sensitivity of the technique to the presence of vacancies, which turned out to be fairly high. On the other hand, little sensitivity is shown by the technique to the in-plane lattice parameter. Few monolayers films were shown to be perfectly strained on the Si(111) surface.[9] The same indications came from EXAFS (Ref. 18) and grazing incidence XRD (Ref. 19) studies of samples with thickness of 200 Å grown in a way similar to that shown in the present paper. In the present XAS analysis for films whose thickness range between 500 and 800 Å, two multiple-scattering calculations with different values of hexagonal lattice constant $a = 3.84$ Å [corresponding to epitaxially strained ErSi$_{1.7}$ on the Si(111) surface] and $a = 3.78$ Å (corresponding to bulk ErSi$_{1.7}$) do not show enough differences to assess the real degree of strain relaxation in the samples. This source of uncertainty could be at the basis of some small discrepancy we observe with models presented in literature.[9] We have to mention that the $R3$ is not the only superstructure observed in bulk silicide phases.[7,8] We chose the $R3$ structural model for the following reasons: it is always found in electron-diffraction studies of bulk films,[7,20] with or without other structures, it is the only one that has been observed so far in surface-sensitive electron-diffraction studies,[2] it corresponds to the x-ray-diffraction results for thin films,[9] and it gives the right composition ErSi$_{1.67}$, close to the experimental values. Additionally, we think that it could represent a reasonable approximation for the local order around Si atoms in more complicated structures that have been observed.[7,8,20] In Figs. 2 and 3, we report the comparisons between theory and experiments for the two main polarization conditions. In Fig. 2 we consider the case of the electric field in the plane of the surface (p_{x-y} final state) and in Fig. 3 the case of the electric-field perpendicular to the surface (p_z final state). In these two figures the experimental curves were background subtracted while theoretical XAS spectra have been computed for the four structures presented above: stoichiometric ErSi$_2$ (no Si vacancies); ErSi$_{1.7}$ with vacancies but without relaxation around the Si vacancies; $R1$ and $R2$ with both Si vacancies and relaxations as described in Sec. III.

We first consider the influence of the vacancies on the spectra. It is immediately clear from Figs. 2 and 3 that the three models that include Si vacancies (labeled ErSi$_{1.7}$, $R1$-ErSi$_{1.7}$, and $R2$-ErSi$_{1.7}$) give a much better account of

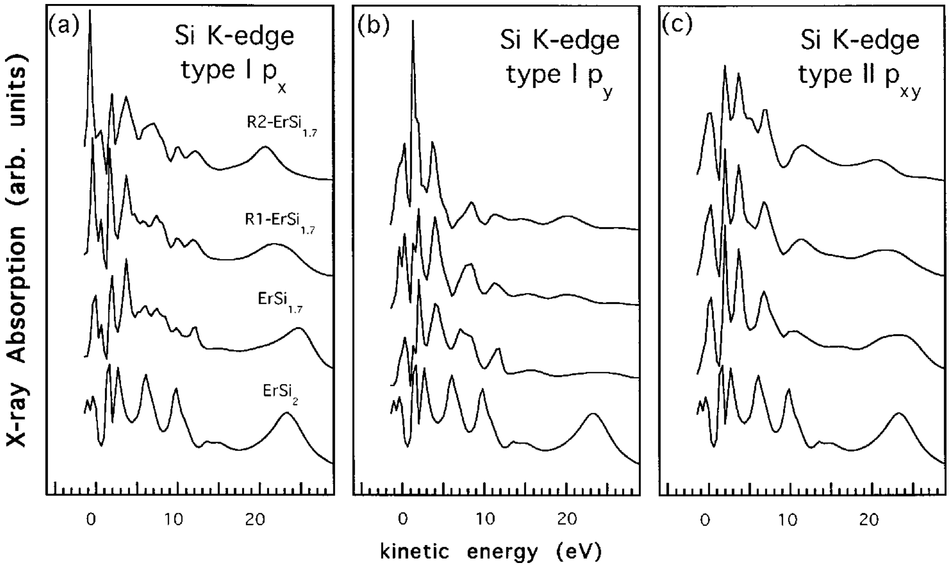

FIG. 4. (a) Theoretical XAS spectra of ErSi$_{1.7}$ Si K edge for p_x final state in the case of type-I absorber Si atoms (absorber atoms with dangling bonds). The electric field is directed perpendicular to the dangling bond. (b) Theoretical XAS spectra of ErSi$_{1.7}$ Si K edge for p_y final state in the case of type-I absorbers. The electric field is directed parallel to the Si dangling bond. (c) Theoretical XAS spectra of ErSi$_{1.7}$ Si K edge for p_{x-y} final state in the case of type-II absorbers (absorber atoms without dangling bonds). In each panel the bottom curve is the stoichiometric case (ErSi$_2$) reported for visual comparison.

the experimental results (upper curves in Figs. 2 and 3) than the model with no vacancies (labeled ErSi_2). The positions and the relative intensities of the main structures of the experimental spectra (indicated by thin vertical lines in Figs. 2 and 3) are not satisfactorily reproduced by spectra computed for stoichiometric ErSi_2. This is clearly seen, for instance, in Fig. 3 where the position of the main maximum of the theoretical spectrum for ErSi_2 is shifted by almost 2 eV towards lower photon energy with respect to the experimental results. The overall agreement with experiment is better for the three spectra computed for structures including vacancies. These results demonstrate quite directly the presence of vacancies in the material, as well as the influence they have on the Si *K* spectrum (this point will be discussed further below).

The amount of relaxation of the various atoms around the vacancy can also be estimated from Figs. 2 and 3 by comparing the three theoretical spectra for $\mathrm{ErSi}_{1.7}$ with the experimental data. From Fig. 3, it appears that the p_z final states are not very sensitive to this relaxation. The same is true for the low-energy part of the p_{x-y} final states in Fig. 2. However, in this latter case, the position of the feature at about 1862 eV varies significantly with the amplitude of the relaxation. The energy of this structure is too high when no relaxation is considered (curve $\mathrm{ErSi}_{1.7}$ in Fig. 2). The agreement with the experiments is better when relaxation is switched on (curves $R1$-$\mathrm{ErSi}_{1.7}$ and $R2$-$\mathrm{ErSi}_{1.7}$ in Fig. 2). The same conclusion, even if less evident, can be drawn in the case of the feature at about 1862 eV in Fig. 3. We note that a nonperfect linear polarization would not affect the present analysis because it relies on the behavior of features of the spectrum which can be straightforwardly addressed to a p_z or a p_{x-y} character.

Although the differences are feeble, it is appreciable that in both cases (spectrum p_{x-y} and p_z) the $R1$-$\mathrm{ErSi}_{1.7}$ structure gives a better account of the actual positions of spectral features than the $R2$-$\mathrm{ErSi}_{1.7}$ spectrum. We can conclude that the XANES Si *K* spectra show that a significant relaxation occurs around the Si vacancies. In this model the Er atoms have two different Si first neighbors at distance 2.97 and 3.04 Å, while Si-Si bond distance is slightly contracted (2.30 Å) with respect to the bulk Si value. The differences found among the structural models taken in consideration are significantly greater than the error on the determination of distances (0.02 Å) of the present technique.

Some information can be also obtained by looking separately at the contributions to the theoretical spectrum, in terms of contribution of absorber of type I, with a dangling bond [Figs. 4(a) and 4(b) for the electric field laying in x-y plane, respectively, perpendicular (p_y) and parallel (p_x) to the dangling bond], and that of absorber type II [Fig. 4(c) for x-y orientation of the electric field] with three first neighbor Si atoms. In all these figures (in which the convolution with broadening functions have not been performed to better put in evidence each feature of the theoretical spectrum) are also reported for comparison the stoichiometric ErSi_2 cases (bottom curves).

In particular if the electric field is directed perpendicular to the dangling bond in type-I absorbers [Fig. 4(a)] a great sensitivity to the relaxation is probed when compared with the case of the electric-field oriented parallel to the dangling bond [Fig. 4(b)]. In the case of type-II absorbers [Fig. 4(c)] less dramatic changes occur at the near edge region of the spectrum for different amounts of relaxation.

We do not report theoretical spectra related to different type absorbers in p_z spectra as no remarkable differences have been observed.

V. CONCLUSIONS

We have investigated the electronic and atomic structure of epitaxial erbium silicide films epitaxially grown on Si(111) by means of XAS at the Si *K* edge. As expected from the crystallographic structure, the spectra show a strong anisotropy as a function of the polarization of the x-ray beam. The data reveal a significant density of Si $3p_{x-y}$ and $3p_z$ states just above the Fermi level in thin material. Comparison with theoretical XANES spectra of several structural models demonstrates the presence of vacancies in the Si planes and clearly shows the occurrence of atomic relaxation around the vacancies. Our results are at least in qualitative agreement with a previous XRD study.[9] The present experimental data and computations should be helpful for future investigations of the electronic structure rare earth silicides, especially for elucidating the role of Si vacancies, and their effects in the electronic density of empty states.

---

[1] F. Arnaud d'Avitaya, A. Perio, J.-C. Oberlin, Y. Campidelli, and J. A. Chroboczek, Appl. Phys. Lett. **54**, 2198 (1989).

[2] D. B. B. Lollman, T. A. Nguyen Tan, J. Y. Veuillen, P. Muret, K. Lefki, M. Brunel, and J. C. Dupuy, Appl. Surf. Sci. **65/66**, 704 (1993).

[3] L. Pahun, Y. Campidelli, F. Arnaud d'Avitaya, and P. A. Badoz, Appl. Phys. Lett. **60**, 1166 (1992).

[4] R. D. Thomson and K. N. Tu, Thin Solid Films **93**, 265 (1982).

[5] J. A. Knapp and S. T. Picraux, Appl. Phys. Lett. **48**, 466 (1986).

[6] F. Arnaud d'Avitaya, P. A. Badoz, Y. Campidelli, J. A. Chroboczek, J. Y. Duboz, and A. Perio, Thin Solid Films **184**, 283 (1990).

[7] F. H. Kaatz, W. R. Graham, and J. Van der Spiegel, Appl. Phys. Lett. **62**, 1748 (1993).

[8] S. Auffret, J. Pierre, B. Lambert, J. L. Soubeyroux, and J. A. Chroboczek, Physica B **162**, 271 (1990).

[9] M. Lohmeier, W. J. Huisman, E. Vlieg, A. Nishiyama, C. L. Nicklin, and T. S. Turner, Surf. Sci. **345**, 247 (1996).

[10] L. Magaud, J.-Y. Veuillen, D. Lollman, T. A. Nguyen Tan, D. A. Papaconstantopoulos, and M. J. Mehl, Phys. Rev. B **46**, 1299 (1992).

[11] L. Magaud, J.-P. Julien, and F. Cyrot-Lackmann, J. Phys.: Condens. Matter **4**, 5399 (1992).

[12] G. Allan, I. Lefebvre, and N. E. Christensen, Phys. Rev. B **48**, 8572 (1993).

[13] L. Stauffer, C. Pirri, P. Wetzel, A. Mharchi, P. Paki, D. Bolmont, G. Gewinner, and C. Minot, Phys. Rev. B **46**, 13 201 (1992).

[14] A. Gheorghiu, C. Sénémaud, E. Belin-Ferré, Z. Dankhazi, L. Magaud-Martinage, and D. A. Papaconstantopoulos, J. Phys.: Condens. Matter **8**, 719 (1996).

[15] T. A. Tyson, K. O. Hodgson, C. R. Natoli, and M. Benfatto, Phys. Rev. B **46**, 5997 (1992), and references therein.

[16] L. Hedin and S. Lundqvist, Solid State Phys. **23**, 1 (1969).

[17] R. A. Rosenberg, P. J. Love, and V. Rehn, Phys. Rev. B **33**, 4034 (1986).

[18] M.-H. Tuilier, C. Pirri, P. Wetzel, G. Gewinner, J.-Y. Veuillen, and T. A. Nguyen Tan, Surf. Sci. **307-309**, 710 (1994).

[19] D. B. B. Lollman, T. A. Nguyen Tan, J. Y. Veuillen, P. Muret, K. Lefki, M. Brunel, and J. C. Dupuy, Appl. Surf. Sci. **65/66**, 704 (1993).

[20] N. Frangis, G. Van Tendeloo, J. Van Landuyt, P. Muret, and T. T. A. Nguyen, J. Alloys Compd. **234**, 244 (1996).